Journal of Catalysis 278 (2011) 228–238

Contents lists available at ScienceDirect

Journal of Catalysis

journal homepage: www.elsevier.com/locate/jcat

Selective hydrogenation of amides using bimetallic Ru/Re and Rh/Re catalysts

Graham Beamson [b], Adam J. Papworth [c], Charles Philipps [a], Andrew M. Smith [a], Robin Whyman [a,*]

[a] Department of Chemistry, Donnan and Robert Robinson Laboratories, University of Liverpool, Liverpool L69 7ZD, UK
[b] National Centre for Electron Spectroscopy and Surface Analysis, STFC Daresbury Laboratory, Warrington, Cheshire WA4 4AD, UK
[c] Materials Science and Engineering, Department of Engineering, University of Liverpool, Liverpool L69 3GH, UK

ARTICLE INFO

Article history:
Received 2 November 2010
Revised 14 December 2010
Accepted 15 December 2010
Available online 26 January 2011

Keywords:
Heterogeneous catalysis
Ruthenium
Rhenium
Rhodium
Bimetallic
Hydrogenation
Amide
Primary amine
Characterization
Reaction mechanism

ABSTRACT

Heterogeneous Ru/Re and Rh/Re catalysts, formed in situ from $Ru_3(CO)_{12}/Re_2(CO)_{10}$ and $Rh_6(CO)_{16}/Re_2(CO)_{10}$ respectively, are effective for the liquid phase hydrogenation of cyclohexanecarboxamide ($CyCONH_2$) to $CyCH_2NH_2$ in up to 95% selectivity without the requirement for ammonia to inhibit secondary and tertiary amine formation. Good amide conversions are noted within the reaction condition regimes 50–100 bar H_2 and $\geqslant$150 (Rh) – 160 °C (Ru). Variations in Ru:Re and Rh:Re composition result in only minor changes in product selectivity with no evidence of catalyst deactivation at higher levels of Re. In situ HP-FTIR spectroscopy has shown that catalyst genesis occurs via decomposition of the metal carbonyl precursors. Ex situ characterization, using XRD, XPS and EDX-STEM, has provided evidence for the active components of these catalysts containing bimetallic Ru/Re and Rh/Re nanoclusters, the surfaces of which become significantly oxidized after use in amide reduction. Potential mechanistic pathways for amide hydrogenation are discussed, including initial dehydration to nitrile, a pathway potentially specifically accessible to primary amides, and evidence for often postulated imine intermediates.

1. Introduction

The generation, characterization and use of bimetallic heterogeneous Rh/Mo and Ru/Mo catalysts for the selective hydrogenation of amides to amines in the liquid phase has recently been described [1,2]. Key features of this work include both high catalyst selectivity for the reduction of primary amides to the respective primary amines, without the necessity for the addition of ammonia and/or amines to inhibit side reactions leading to secondary and tertiary amine by-products, and considerably milder reaction conditions relative to those required by standard first generation copper chromite catalysts [3]. Catalyst performance was shown to be crucially dependent on Mo:Rh and Mo:Ru composition, respective ratios of >2 and >1 leading to either significant, or complete, inhibition of catalysis.

Rhenium-based catalysts have received greater attention than Rh, Ru or Mo for the reduction of 'difficult' functional groups such as amides, and particularly carboxylic acids and esters. Broadbent et al. [4] described the use of Re_2O_7 as a catalyst precursor for the hydrogenation of carboxylic acids under the severe reaction conditions (312 bar H_2, 217 °C, 6 h) typically required by copper chromite catalysts. A step change was described in 1990 by Yoshino et al. [5] with a report of the use of promoted bimetallic Re/Os catalysts under considerably milder reaction conditions (25–100 bar H_2, 100–120 °C, 6 h), with highest alcohol selectivities being favoured at the highest pressure. A subsequent very recent development is the use of titania-supported Pt (and Pt/Re) catalysts with optimum reaction conditions at 20 bar H_2 and 130 °C, although very low reaction rates at as low as 5 bar H_2 and 60 °C are also quoted [6]. The first account of the use of Re in amide reduction was also provided by Broadbent et al. [7], who described the use of Re(VI) oxide for the selective hydrogenation of benzamide to benzylamine (205 bar H_2, 220 °C, 49 h, ethanol solvent) in 69% yield, with toluene as the only by-product. Surprisingly, the formation of neither cyclohexylamine nor N-ethyl-substituted secondary or tertiary amine derivatives were reported [cf. Ref. [2]]. Subsequently, a BP patent claimed the use of a Pd/Re/high surface area graphite/zeolite 4A combination, dispersed in a solvent such as 1,4-dioxane, for the reduction of amides at 130 bar H_2 and 200 °C [8]. Using propionamide as substrate, the product distribution comprised a mixture of primary, secondary and tertiary amines. Fuchikami et al. [9] briefly described the behaviour of Rh/Re catalysts for the reduction of a range of amides. In the one example of a primary amide tested, *n*-hexanamide required the co-addition of an amine (diethylamine) to induce good selectivity to *n*-hexylamine under reaction conditions of 100 bar H_2 and 180 °C. Otherwise di(*n*-hexyl)amine comprised the predominant

* Corresponding author. Fax: +44 (0) 151 794 3588.
E-mail address: whyman@liv.ac.uk (R. Whyman).

0021-9517/$ - see front matter © 2010 Elsevier Inc. All rights reserved.
doi:10.1016/j.jcat.2010.12.009

product, in complete contrast to our recent findings with Rh/Mo and Ru/Mo catalysts using cyclohexanecarboxamide ($CyCONH_2$) as substrate [1,2]. Here, the genesis and performance of both Ru/Re and Rh/Re catalysts in the hydrogenation of $CyCONH_2$ (and *N*-acetylpiperidine) are reported, together with ex situ characterization using microanalysis, XRD, XPS and EDX-STEM.

2. Materials and methods

With the exception of the additional details described below, experimental and analytical procedures are as outlined in Refs. [1,2].

2.1. Reagents

$Re_2(CO)_{10}$ (98%) was purchased from Strem Chemicals and the XPS standard, Re foil (0.025 mm thickness, 99.98%), from Aldrich Chemicals.

2.2. Catalytic procedures

A typical 'single-pot' batch Ru/Re catalyst preparation, and evaluation in $CyCONH_2$ reduction, was carried out as follows, for a nominal Re:Ru atomic composition of 0.25. [$Ru_3(CO)_{12}$] (22 mg, 0.103 mmol Ru), [$Re_2(CO)_{10}$] (8.4 mg, 0.026 mmol Re) and cyclohexanecarboxamide (0.235 g, 1.85 mmol) contained in a glass liner were dissolved in 1,2-dimethoxyethane (DME) (30 mL) and *n*-octane (0.100 g) added as an internal standard for GC analysis. The liner was placed in a ca. 300-mL capacity pressure vessel and the reaction mixture, under agitation, purged three times with N_2 (at 5 bar), and three times with H_2 (5 bar). The autoclave was then pressurized to 100 bar H_2 and heated to 160 °C for 16 h. A very dark coloured liquid was initially recovered after cooling and venting and from this a black residue slowly settled, leaving a colourless solution. The residue was separated by centrifugation (2000 rpm, 20 min) and the supernatant liquid containing reaction products removed. After several washings with DME (10 mL), the catalyst residue (ca 15 mg) was dried and the resultant fine black powder either recycled using the same quantities of fresh substrate and solvent, or characterized using the techniques described below. Product solutions were analysed by GC as previously described [1].

In addition to 'batch' experiments, 'parallel' catalyst evaluations were also conducted. A typical 'parallel' catalyst evaluation was carried out using the standard autoclave used for batch runs, modified to accommodate four vertically mounted modified test tubes of ca. 20 mL capacity, all containing mini-magnetic followers to ensure effective stirring. Using a 10 mL volume of DME solvent, the scale of substrate and catalyst precursors (4 mol% Ru) were reduced accordingly.

2.3. Ex situ characterization

2.3.1. EDX-STEM

Sample quantification was determined using the most intense 'pure' Ru K 1α (19.279 keV) and Re L 1α (8.654 keV) lines that are largely free from interference by signals from other elements. Even so, both trace O and Si were also detected during the analysis and deconvolution of the Si K and Re L lines became necessary for accurate quantification. Also, since Ru K and Re L lines are under comparison, the quoted values are subject to an error of ±5%.

2.3.2. Microanalyses

All elemental analyses were performed by Mr. S.G. Apter, Department of Chemistry, University of Liverpool. Transition metal concentrations were determined using a Spectro Ciros CCD Inductively Coupled Plasma (ICP) source linked to Atomic Emission Spectroscopy (AES). Sample digestion was accomplished using a matrix combination containing aqua regia (2 eq. HCl: 1 eq. HNO_3) (5 mL) and HF (0.5 mL), followed by microwave treatment in a CEM MARS5 oven using the following programme conditions; heating to 220 °C at 20 °C min^{-1}, holding at 220 °C for 20 min followed by a cooling period of 20 min. The resultant solutions were diluted to 100 mL in distilled water and referenced against Ru, Rh and Re standards made up in similar HCl/HNO_3/HF matrix solutions. Application of this procedure overcame the well-known resistance of Ru in particular to digestion [10] (see Supplementary material S2 for further details).

Standard C, H and N determinations were carried out by combustion analysis using either a Flash EA-1112 or a Model 1106 Carlo Erba thermal elemental analyzer at ~2000 °C. For the bimetallic catalyst samples, a V_2O_5 catalyst was required to aid combustion.

3. Results and discussion

3.1. N-acetylpiperidine hydrogenation using Ru/Re catalysts

A hydrogenation catalyst derived from $Ru_3(CO)_{12}$ and $Re_2(CO)_{10}$ (Re:Ru = 1.0, 1 mol% Ru) was reported by Fuchikami et al. [9] to give high conversions of *N*-acetylpiperidine into *N*-ethylpiperidine (96% yield) under standard reaction conditions of 100 bar H_2 and 160 °C. Ru alone was essentially inactive (1% conversion and amine yield) and Re showed low activity (14% conversion) with only 7% yield of the desired amine. Repetition of this work using $Re_2(CO)_{10}$ has confirmed reproducibility (16% conversion, 53% amine selectivity) and revealed that competing C—N bond hydrogenolysis of *N*-acetylpiperidine (to ethanol and piperidine) accounts for the additional products. No attempts to use Ru/Re catalysts for the reduction of primary amides such as cyclohexanecarboxamide, $CyCONH_2$, have been reported and this has provided the focus for our work.

3.2. $CyCONH_2$ hydrogenation using Ru/Re catalysts

3.2.1. Variation of Re:Ru composition

Using a series of parallel experiments (10 mL scale and 4 mol% catalyst, based on Ru), the results of variation in Re:Ru ratio are shown in Fig. 1. From this, it is evident that the addition of only a small concentration of $Re_2(CO)_{10}$ to $Ru_3(CO)_{12}$, comparable to that observed with Ru/Mo (and Rh/Mo) catalysts, is necessary to initiate analogous overall conversion/product selectivity synergy. In contrast however there is no evidence of significant reduction in conversion with increasing Re content, for up to Re:Ru = 1.8. Moreover, product selectivity remains essentially constant between Re:Ru values of 0.25 and 1.1, with uniformly trace amounts of $(CyCH_2)_2NH$ present across the range Re:Ru = 0.3–1.8, and only at Re:Ru = 1.8 are slight divergences of product distribution in favour of $CyCH_2OH$ apparent. A Re:Ru composition of ca. 0.3 appears optimum for a combination of conversion and selective formation of $CyCH_2NH_2$ (both >90%). The conversion and selectivity recorded for the Re:Ru = 0.34 catalyst in Fig. 1 are those obtained from the final reaction solution from the in situ HP-FTIR experiment using the complete $CyCONH_2$ reduction system, described in Section 3.6.1, thus confirming internal consistency between the two sets of experimental data.

Furthermore, for the purposes of checking reproducibility between 'parallel' and 'batch' processing, three Ru/Re catalysts were examined in batch experiments, using 5 mol% Ru. The results summarized in Table 1 provide confirmation, with essentially the same reaction product profile and only a marginal improvement in

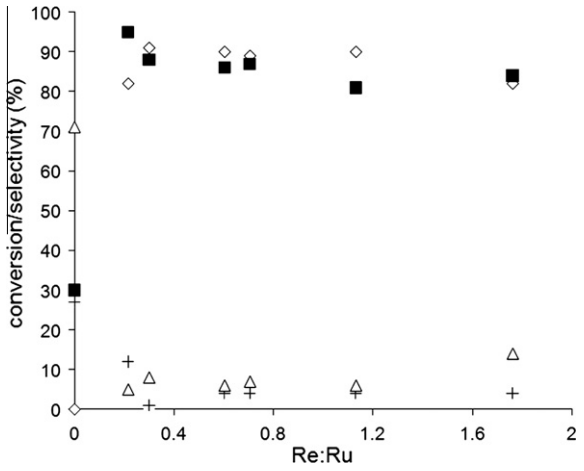

Fig. 1. $CyCONH_2$ hydrogenation: (a) overall conversion and (b) product selectivity vs. Re:Ru composition (100 bar H_2, 160 °C, 16 h). Key: ■ Conversion, ◇ $CyCH_2NH_2$, + $(CyCH_2)_2NH$, △ $CyCH_2OH$.

selectivity towards $CyCH_2NH_2$. No secondary amine production is evident with Re:Ru = 0.34 and 0.54 catalysts (Entries 2 and 3) and only traces at Re:Ru = 0.15 (Entry 1), in which the $CyCH_2NH_2/CyCH_2OH$ product distribution is a close parallel with that observed with Ru/Mo catalysts of equivalent composition [2].

3.2.2. Variation of total catalyst concentration

A preformed Ru/Re (Re:Ru = 0.25) catalyst previously prepared in the absence of the amide substrate was used, in batch experiments, to establish a conversion/selectivity profile for $CyCONH_2$ reduction as a function of total catalyst concentration. The results (Table 2 and Supplementary material Fig. S1) show that $CyCH_2NH_2$ selectivity (93–96%) is essentially unaffected and that amide conversion displays an approximately first-order dependence on catalyst concentration. Hence, an apparent discrepancy between the incomplete amide conversions evident throughout the 'parallel' experiments shown in Fig. 1, and the 100% conversions noted in Table 1, may be rationalized in terms of the slightly higher (5 vs. 4 mol%) Ru catalyst concentration used in the batch experiments.

3.2.3. Variation of pressure and temperature

The effects of variation in pressure and temperature on $CyCONH_2$ hydrogenation during batch experiments are summarized in Table 3. From this data, it is clear that the standard reaction conditions of 100 bar H_2 and 160 °C are necessary for highest $CyCH_2NH_2$ selectivity, which undergoes a significant reduction at 50 bar H_2, notwithstanding essentially complete $CyCONH_2$ conversion (cf. Entries 1 and 2). Reduction in reaction pressure to 20 bar H_2 (Entry 3) results in much lower amide conversion, a further slight reduction in selectivity towards $CyCH_2NH_2$, and increased $(CyCH_2)_2NH$ production. Furthermore, reaction temperatures below 160 °C are also clearly deleterious to catalytic performance, with 20% conversion at 150 °C (Entry 4) and zero activity evident at 140 °C (Entry 5). This behaviour contrasts markedly with the limiting parameters of 20 bar H_2/160 °C and/or 100 bar H_2/130 °C

Table 1
$CyCONH_2$ hydrogenation. Dependence of conversion and product distribution on Re:Ru composition in batch experiments.

Entry	Re:Ru	Conversion (%)	Product selectivity (%)		
			$CyCH_2NH_2$	$CyCH_2OH$	$(CyCH_2)_2NH$
1	0.15	100	86	12	Trace
2	0.34	100	92	7	0
3	0.54	100	93	6	0

Reaction conditions: 100 bar H_2, 160 °C, 16 h, 5 mol% Ru.

Table 2
$CyCONH_2$ hydrogenation. Dependence of conversion and product distribution on catalyst concentration.

Catalyst concentration (mol%)	Conversion (%)	Product selectivity (%)		
		$CyCH_2NH_2$	$CyCH_2OH$	$(CyCH_2)_2NH$
4.0	90	95	3	2
2.2	50	93	6	1
1.2	32	96	3	<1

Reaction conditions: 100 bar H_2, 160 °C, 16 h, Re:Ru = 0.25 catalyst.

Table 3
$CyCONH_2$ hydrogenation: conversion and product selectivity vs. pressure and temperature.

Entry	T (°C)	P_{H2} (bar)	Conversion (%)	Product selectivity (%)		
				$CyCH_2NH_2$	$CyCH_2OH$	$(CyCH_2)_2NH$
1	160	100	95	91	8	1
2	160	50	98	81	16	3
3	160	20	60	77	13	9
4	150	100	20	80	17	2
5	140	100	0	–	–	–

Reaction time:16 h, Re:Ru = 0.25 catalyst.

available to Ru/Mo catalysts [2]. Any potential explanation in terms of decreased availability of H_2 in DME solution at the lower pressures using Ru/Re catalysts seems therefore to be unlikely (for further information on H_2 solubility in DME, see Supplementary material S1, Table S1 and Figs. S2 and S3).

3.3. N-acetylpiperidine hydrogenation using Rh/Re catalysts

In a preliminary single-pot reaction using *N*-acetylpiperidine as substrate, a Rh/Re catalyst (Re:Rh = 1.0, 1 mol% Rh) derived from $Rh_6(CO)_{16}$ and $Re_2(CO)_{10}$ gave >80% conversion to *N*-ethylpiperidine in >85% selectivity, using the standard reaction conditions of 100 bar H_2, 160 °C and 16 h, in confirmation of the report of Fuchikami et al. [9]. As found with the Rh/Mo [1] and Ru/Mo [2] catalysts, the solid material generated during this single-pot reaction could be recovered most easily from the product solution by centrifugation, repeated washing with DME solvent, and subsequent drying. Following re-charging with *N*-acetylpiperidine after this treatment catalyst recycle could be conveniently monitored using HP-FTIR spectroscopy, by following the decay of the amide carbonyl absorption band at 1658 cm^{-1} as a function of time (see Supplementary material, Fig. S4), from which it is clear that initiation of hydrogenation occurs without an induction period on reaching the operational temperature of 160 °C (at time = 0 min).

3.4. $CyCONH_2$ hydrogenation using Rh/Re catalysts

In Fuchikami's work [9], the one experiment reporting the use of a primary amide (*n*-hexanamide), at a Re:Rh composition of 2, required the addition of an amine (diethylamine) to induce good selectivity to the primary amine. This contrasts with our more recent results using Rh/Mo, Ru/Mo and Ru/Re catalysts prepared in a similar manner, in which the addition of neither ammonia nor amine is required for high primary amine selectivity. Our standard substrate $CyCONH_2$ was therefore used to determine whether Rh/Re catalysts do indeed exhibit fundamentally different behaviour towards the reduction of primary amides.

3.4.1. Variation of Re:Rh composition

Results of variation in Re:Rh composition on $CyCONH_2$ hydrogenation are shown in Fig. 2, from which it is evident that in contrast to Ru/Re catalysts (also Rh/Mo and Ru/Mo), the sequential addition

of Re to Rh only leads to a gradual increase in conversion over the Re:Rh range 0–0.67, and quite possibly beyond. Consequently, a more substantial concentration of Re (ca. Re:Rh = 0.7) is required for 100% $CyCONH_2$ conversion. Nevertheless, $CyCH_2NH_2$ is still the major product throughout, formed in 90% selectivity using a Re:Rh = 0.80 catalyst composition. These results provide a distinct contrast with that of Fuchikami et al. [9] and confirm our belief that high primary amine selectivities comprise an intrinsic characteristic of all the bimetallic systems investigated (Ru/Mo, Ru/Re, Rh/Mo and Rh/Re), at least when using $CyCONH_2$ as a primary amide substrate. Nevertheless, in displaying a gradual increase in conversion as a function of Re content, the Rh/Re catalysts clearly differ in relation to the degree of synergism that was so clearly evident, and necessary, for the high amide conversions and primary amine selectivities associated with the first three members of the series.

3.4.2. Variation of amide concentration

Using batch experiments, the dependence of amide concentration on reaction selectivity, using a Re:Rh = 0.80 catalyst composition (5 mol% Rh), are shown in Table 4, from which it is clear that high dilution is beneficial, with the highest selectivity towards $CyCH_2NH_2$ occurring at the lowest amide concentration (Entry 1), the standard concentration used in all the Re:Rh, pressure and temperature variation experiments (see Section 3.4.3). The increased amount of secondary amine formation in solutions containing higher amide concentrations is presumably a consequence of the greater probability of condensation reactions occurring on the catalyst surface. In contrast, $CyCH_2OH$ formation remains largely constant throughout.

3.4.3. Variation of pressure and temperature

Using a Re:Rh = 0.80 catalyst and standard batch experiments, the results of the effects of variation in pressure and temperature on $CyCONH_2$ hydrogenation are summarized in Table 5. Although high amide conversions are maintained at 50 bar H_2 (Entry 2), a significant reduction of primary amine selectivity in favour of $(CyCH_2)_2NH$, relative to that noted at 100 bar (Entry 1) is evident, $CyCH_2OH$ remaining unchanged. A considerable reduction in conversion is noted at 20 bar (Entry 3), with selectivity towards $CyCH_2OH$ significantly increased in relation to that at 50 bar, notwithstanding a minor increase in $(CyCH_2)_2NH$ formation. Inspection of Entries 4–6 shows that any reduction in reaction temperature below 150 °C is deleterious to catalyst performance, with no reaction evident at 130 °C during the standard 16 h reaction time. Nevertheless, slow reduction does occur during a considerably extended reaction time (Entry 7). This could possibly be a consequence of lower rates of $Re_2(CO)_{10}$ decomposition, and active catalyst formation, at 130 °C. Overall, reaction conditions of 100 bar H_2 and 160 °C (cf. Entry 1) do appear necessary to give a combination of the highest amide conversions and primary amine selectivities.

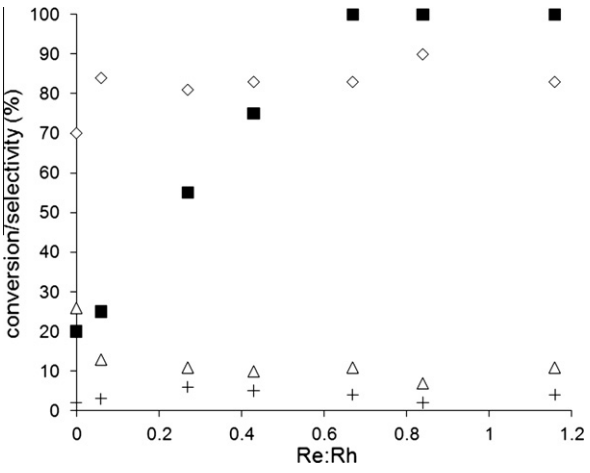

Fig. 2. $CyCONH_2$ hydrogenation: (a) conversion and (b) product selectivity vs. Re:Rh composition (100 bar H_2, 160 °C, 16 h). Key: ■ Conversion, ◇ $CyCH_2NH_2$, + $(CyCH_2)_2NH$, △ $CyCH_2OH$.

Table 4
$CyCONH_2$ hydrogenation. Variation of conversion and product selectivity with amide concentration.

Entry	Amide (mol/L)	Conversion (%)	Product selectivity		
			$CyCH_2NH_2$	$CyCH_2OH$	$(CyCH_2)_2NH$
1	0.072	97	89	3	7
2	0.112	100	80	6	11
3	0.147	100	82	6	11
4	0.181	93	74	6	18

Reaction conditions: 100 bar H_2, 160 °C, 16 h, Re:Rh = 0.80 catalyst.

3.5. Similarities and differences in catalyst behaviour

From the results described earlier, it appears that Ru/Re and Rh/Re catalysts both provide excellent intrinsic selectivities for the reduction of $CyCONH_2$ to $CyCH_2NH_2$. Although they are actually superior in terms of primary amine selectivity, the minimum pressure and temperature requirements (cf. Tables 3 and 5, Entry 1) dictate the use of 100 bar H_2 and 160–150 °C, respectively, for good amide conversions, and in this respect, they are of inferior performance to their Ru/Mo and Rh/Mo counterparts. With Ru/Re catalysts, an increase in the concentration of Re above the threshold value of ca. Re:Ru = 0.15 has little effect on catalyst selectivity, although there is a general trend of decreasing conversion and increased secondary amine production at higher Re:Ru catalyst loadings. With the Rh/Re systems, low initial concentrations of Re enhance the high primary amine selectivity above that observed with the base Rh case (70%, Fig. 2), but additional Re content is necessary to allow 100% $CyCONH_2$ conversion under the standard reaction conditions, cf. Fig. 2.

3.6. Catalyst genesis using in situ HP-FTIR spectroscopy

3.6.1. Ru/Re catalysts

Inspection of absorbances of the amide carbonyl band at 1693 cm^{-1} in spectra of the complete $CyCONH_2$ amide reduction system, using $Ru_3(CO)_{12}$ and $Re_2(CO)_{10}$ (Re:Ru = 0.34) as catalyst precursors, and a standard heating time of ca. 15 min to 160 °C (see Supplementary material Fig. S5, first entry at 160 °C shown as time = 0 min), reveals that amide reduction commences immediately on reaching the operational reaction temperature. Calculated as previously described [2], the amide decay curve corresponds to an initial TON (mmol. $CyCONH_2$ consumed vs. mmol. Ru) of 1.9 h^{-1}. Thus, in sharp contrast to Rh/Re catalysts (see Section 3.6.2) and to the Rh/Mo and Ru/Mo catalyst systems described previously [1,2], no catalyst induction period appears necessary for this combination. All evidence of $Ru_3(CO)_{12}$ disappears during the initial heating period, and the residual ν(CO) absorptions, corresponding with the spectrum of $Re_2(CO)_{10}$, slowly degrade during the subsequent 2 h.

A control experiment, also using a 0.34 Re:Ru precursor ratio but with stepped, rather than continuous heating (see Fig. 3), provides some amplification of the initial stages of catalyst genesis. At room temperature, both Ru and Re precursors are clearly identifiable by comparison with dominant features of reference spectra, cf. $Ru_3(CO)_{12}$ (2062 cm^{-1}), $Re_2(CO)_{10}$ (2069, 2014 and 1971 cm^{-1}). On heating to 80 °C, the 2062-cm^{-1} band has been displaced by absorptions at 2036 and 2000 cm^{-1}, consequent upon the formation of $[H_3Ru_4(CO)_{12}]^-$, as found in the Ru/Mo systems [2]; the

Table 5
$CyCONH_2$ hydrogenation: conversion and product selectivity vs. pressure and temperature (Re:Rh = 0.80 catalyst).

Entry	T (°C)	P_{H2} (bar)	Conversion (%)	Product selectivity (%)		
				$CyCH_2NH_2$	$CyCH_2OH$	$(CyCH_2)_2NH$
1	160	100	98	90	6	3
2	160	50	98	78	7	13
3	160	20	61	69	14	17
4	150	100	97	84	8	6
5	140	100	64	83	8	7
6	130	100	0	–	–	–
7[a]	130	100	60	81	9	6

Reaction time: 16 h, Re:Rh = 0.80 catalyst.
[a] Reaction time 68 h.

additional absorption expected at 2018 cm^{-1} being masked by the intense band due to $Re_2(CO)_{10}$. All Ru-containing species decompose before 160 °C is reached, at which point ca. Thirty percentage of the $Re_2(CO)_{10}$ initially charged remains in solution. A combination of 70% of the $Re_2(CO)_{10}$ initially present with complete decomposition of $Ru_3(CO)_{12}$ would in fact correspond to a catalyst comprising the optimum Re:Ru value of 0.25 (cf. Fig. 1). Consequently, decomposition of the remaining 30% of $Re_2(CO)_{10}$ during the subsequent 2-h period shown in Fig. 3, throughout which slow reduction of $CyCONH_2$ is taking place, may be largely superfluous to overall catalyst performance. It may indeed be deleterious, since inspection of Fig. 1 reveals a slight decrease in conversion with increasing Re content, which may be a reflection of the onset of the considerably more extensive catalyst poisoning previously encountered with the Ru/Mo and Rh/Mo catalyst systems. The greater stability of $Re_2(CO)_{10}$, relative to $Ru_3(CO)_{12}$, with respect to decomposition is entirely consistent with the position of Re (comprising a third row transition element) in the Periodic Table. Thus, the situation is not directly comparable to that in which $Mo(CO)_6$ was used as co-catalyst precursor with $Ru_3(CO)_{12}$, and where the former species was found to be the first component to undergo rapid decomposition [2].

The results of a further control experiment, namely the reaction of H_2 with a DME solution of $Re_2(CO)_{10}$ alone under the standard amide reduction conditions, are also revealing. Here, full decomposition of the organometallic molecule to metallic Re does not occur during the standard 16-h reaction period, in which $Re_2(CO)_{10}$ is converted, possibly via $H_4Re_4(CO)_{12}$ (ν(CO) 2042s, 1990 m cm^{-1}) [11] in the O-donor solvent, into $Re_4(OH)_4(CO)_{12}$ (ν(CO) 2027s and 1923br cm^{-1}) [12], which could be recovered in the form of a clear pale yellow solution after cooling and depressurization. Furthermore, from an inspection of the relative band intensity ratios associated with the spectrum of $Re_2(CO)_{10}$, there is no evidence for the intermediate formation of significant amounts of $HRe(CO)_5$ (ν(CO) 2015s and 2006 m cm^{-1}) [13] during the reaction of H_2 with $Re_2(CO)_{10}$ at 100 bar H_2 and 160 °C.

In summary therefore, the presence of both $Ru_3(CO)_{12}$ and subsequent reaction products, e.g., $[H_3Ru_4(CO)_{12}]^-$ appear to initiate and enhance partial decomposition of $Re_2(CO)_{10}$ during the initial stages of catalyst genesis. Onset of catalytic activity appears to be dependent only on complete decomposition of the Ru carbonyl intermediates, which occurs very rapidly, and is largely independent of the overall rate of decomposition of $Re_2(CO)_{10}$.

3.6.2. Rh/Re catalysts

In situ HP-FTIR spectra of the Rh/Re systems (Fig. 4) were less conclusive than those of Ru/Re in terms of identifying a parallel effect, namely the role of Rh carbonyl decomposition in initiating and enhancing decomposition of $Re_2(CO)_{10}$ during catalyst genesis, simply because the decay of ν(CO) absorption bands associated with $Rh_6(CO)_{16}$ could not be readily identified due to its limited solubility in DME. Nevertheless, a peak at 1755 cm^{-1} may correspond with the formation and presence of either polynuclear Rh carbonyl anions such as $[Rh_6(CO)_{15}]^{2-}$ [14], or $[Rh_{13}(CO)_{24}H_x]^{n-}$ ($x = 2$, $n = 3$; $x = 3$, $n = 2$, etc.), the carbonyl hydride-containing family proposed in the Rh/Mo catalyst precursor systems [1]. Significant differences from the Ru/Re systems are however readily evident. Genesis of a Rh/Re (Re:Rh = 1) catalyst, chosen on the basis of the information in Fig. 2 to be above the threshold of 0.8 for complete amide hydrogenation under the standard reaction conditions, requires an induction period of ca. 500 min, with initiation apparently dependent on complete decomposition of $Re_2(CO)_{10}$, a situation in close parallel to that observed with Rh/Mo catalysts [1] (cf. Fig. 4, in which ν(CO) absorptions at 2069, 2014 and 1971 cm^{-1} correspond to the presence of $Re_2(CO)_{10}$). Internal consistency with catalyst performance as a function of Re:Rh (cf. Fig. 2) is also evident.

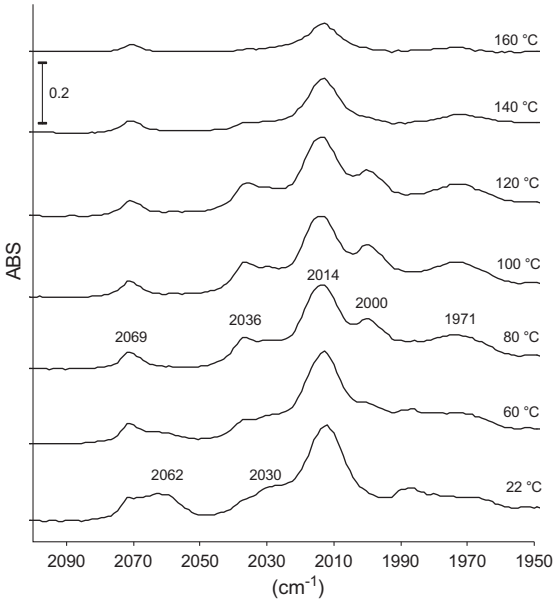

Fig. 3. In situ HP-FTIR spectra (2100–1950 cm^{-1}) during initial stages of catalyst genesis. Reaction conditions: 100 bar H_2, 22–160 °C, Re:Ru = 0.34 catalyst, DME solvent.

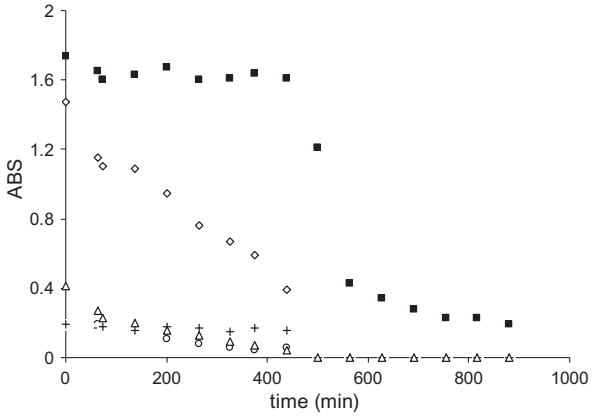

Fig. 4. In situ HP-FTIR spectra (2100–1600 cm^{-1}) showing decay and disappearance of ν(CO) absorptions during catalyst genesis followed by initiation of hydrogenation. Reaction conditions: 100 bar H_2 and 160 °C, Re:Rh = 1 catalyst. Key: ■ $CyCONH_2$ (1693 cm^{-1}), ◇ 2014 cm^{-1}, △ 2069 cm^{-1}, ○ 1971 cm^{-1}, + 1755 cm^{-1}.

3.7. Ex situ catalyst characterization

3.7.1. XRD

3.7.1.1. Ru/Re catalyst. The XRD profile of a Ru/Re (Re:Ru = 0.23) composition, representative of an active and highly selective catalyst, is shown in Fig. 5. As might be expected, given the above stoichiometry, the diffractogram appears dominated by the profile of metallic Ru. Unfortunately, the most intense 2θ = 43.98, 47.35 and 50.29° lines expected for metallic Re [15] are largely obscured by the Ru diffraction pattern. However, by analogy with the Ru/Mo and Rh/Mo catalysts, where the bulk of the Mo was found to be amorphous, and in the oxidized form, it is possible that a similar situation may arise with the Re component of the Ru/Re catalysts. The most intense 'Ru' (1 0 1) line at 2θ = 51.54° corresponds to a *d*-spacing of 2.059 Å (cf. 2.056 Å for Ru metal), and thus any significant lattice expansion associated with incorporation of Re into the Ru lattice, as observed and tentatively suggested for Mo in the Ru/Mo systems [2], is not evident here. Moreover, application of the Scherrer equation to the Ru 2θ lines at 51.54 and 94.35° [Ru (1 0 3)], respectively, of which the latter is most free of interference from Re, gives average crystallite sizes of 8.4 and 8.5 nm. These values are closely comparable with that (8.2 nm) found previously for metallic Ru derived from $Ru_3(CO)_{12}$ alone, material which proved to be a very poor catalyst for $CyCONH_2$ hydrogenation [2]. These results are however consistent with in situ HP-FTIR observations during catalyst genesis, where decomposition of the $Ru_3(CO)_{12}$ precursor was found to occur largely prior to, and partially independently of, $Re_2(CO)_{10}$.

3.7.1.2. Rh/Re catalyst. The diffractogram of a Re:Rh = 0.78 catalyst, shown in Fig. 6, appears consistent with the presence of both metallic Rh and Re, the latter comprising a minor component which again may be partly in the amorphous, presumably oxidized form (see Section 3.7.1.1). The profile is significantly broader than that of metallic Rh derived from $Rh_6(CO)_{16}$ alone, for which a mean crystallite size of 10.6 nm was estimated [1]. Application of the Scherrer equation to the Rh (2 2 0) 2θ line at 83.37° gives a mean crystallite size of 3.8 nm, a similar value to those found for Rh/Mo (and Ru/Mo) catalysts and apparently in sharp contrast to the Ru/Re system.

3.7.2. EDX-STEM of Ru/Re catalyst (Re:Ru = 0.15)

A fresh catalyst of composition Re:Ru = 0.15 was examined using EDX-STEM, with an EDX spectrum to confirm the purity of the sample, and several different areas were mapped. Fig. 7 shows, in high magnification, the bright field image of an aggregate of particles in one typical area, in which individual particle sizes are estimated to lie within the range ca. 2–4 nm. Individual Ru K and Re L maps are shown in Fig. 8a and b, respectively; their comparison showing clearly that wherever Ru is detected, Re is also present, thus confirming the close association between Ru and Re; Re alone is also evident, in much lower concentrations, distributed across other areas of the sample, the homogeneous mixing providing a close parallel with the Ru/Mo and Rh/Mo catalysts. Quantification of the constituent elements, selected by particle density, over areas of the micrograph highlighted in green, Fig. 8c–e shows that the Re:Ru atomic composition is largely homogeneous (ca. 19:81 at.%) throughout, notwithstanding the greater error inherent in the smaller area of analysis (e) which compares reasonably well with the expected Re/Ru at.% composition of 15/85 based on microanalysis. For a rationalization of the apparent discrepancy between the XRD data (Section 3.7.1.1) and these EDX-STEM results, see Section 4.

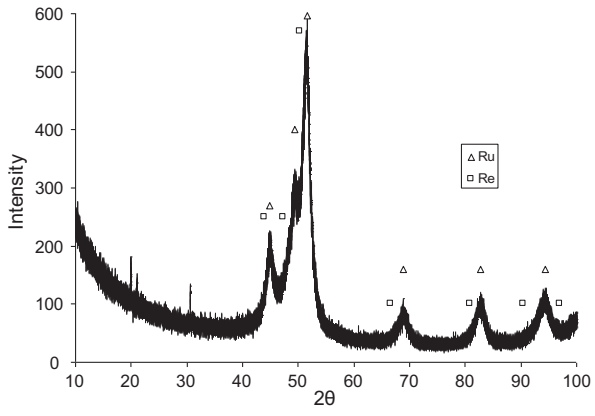

Fig. 5. XRD profile of a fresh Ru/Re catalyst (Re:Ru = 0.23), including reference Ru and Re metal 2θ data points.

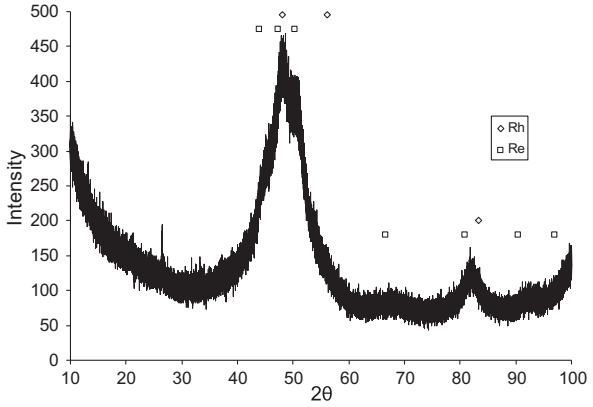

Fig. 6. XRD profile of a fresh Rh/Re catalyst (Re:Rh = 0.78), including reference Rh and Re 2θ metal data points.

3.7.3. XPS

3.7.3.1. Ru/Re catalysts. XPS data were recorded for two catalysts, Re:Ru = 0.12 and 0.54, both before and after Ar^+ sputter etching, the former after use in cyclohexene hydrogenation, and the latter after recycle following a single-pot $CyCONH_2$ hydrogenation. Assignment of the spectra was complicated by both the superimposition of C1s and Ru $3d_{3/2}$ lines at ca. 280 eV, and the 'Re 4f' spectral envelope comprising a composite of Re 4f (major) and Ru 4p (minor) components. Both catalysts showed a dominant Ru ($3d_{5/2}$) peak at 280.1 eV, consistent with the metallic Ru(0) state, together with a slight asymmetry on the high energy side that reduced during Ar^+ sputter etching. The asymmetry could be attributed to the presence of either RuO_2 (280.7 eV) and/or C (280.4 eV). Application of curve fitting procedures (details of which for both these and Rh/Re catalysts, see Section 3.7.3.2, are described in Supplementary material S3), to the 'Re 4f' envelopes (Figs. 9 and 10), allowed the Re and Ru components to be resolved; quantification data for M:Re (M = Ru or Rh) and Re valence state distributions are summarized in Table 6.

After curve fitting, the composite spectrum of the Re:Ru = 0.12 catalyst (Fig. 9) was found to be consistent with three components, namely two distinct Re ($4f_{7/2}$) lines at 40.3 and 41.4 eV (**1** and **3** respectively), of which the former may be readily assigned to Re metal by comparison with reference standards [16] and the third, a Ru ($4p_{3/2}$) line (**5**) at 43.1 eV, also assigned to the metallic state. The second Re ($4f_{7/2}$) component at 41.4 eV clearly corresponds to an oxidized valence state of Re, and chemically, the sesquioxide Re_2O_3 [17] appears a likely possibility, although no XPS measurements are available for this material. Support for the suggestion of a Re(III) valence state is however provided by a Re ($4f_{7/2}$) binding

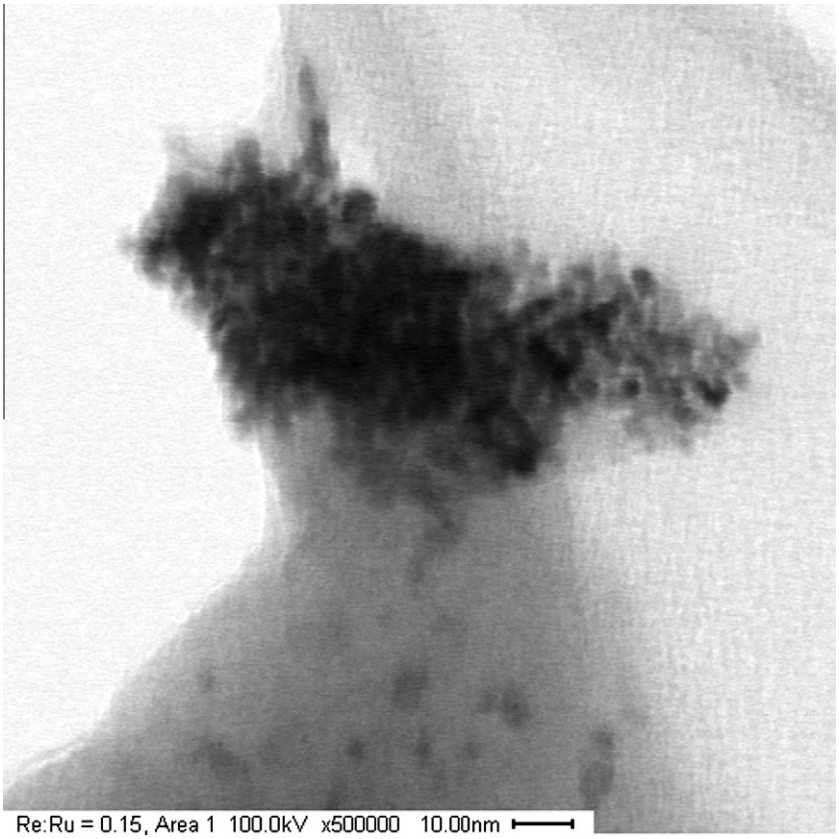

Fig. 7. EDX-STEM analysis: bright field image of typical area of Re:Ru = 0.15 catalyst.

energy of 41.8 eV reported for the complex $[ReCl_3(PMe_2Ph)_3]$ [18]. For comparison, ReO_2, ReO_3 and Re_2O_7 have ($4f_{7/2}$) binding energies of 42.3, 44.3 and 46.7 eV, respectively [16].

The result of curve fitting of the spectrum of the Re:Ru = 0.54 catalyst (Fig. 10) provides a distinct contrast, revealing no fewer than five Re valence states [Re ($4f_{7/2}$) lines **1**, **3**, **5**, **7** and **9**, respectively], comprising Re(0) and Re (III, IV, VI, and VII) (see Table 6). Because of the higher Re content in this sample, the Ru 4p components were considered to be too small to be meaningful. The oxidized valence states, most notably Re(VII), also appeared resistant to removal by Ar^+ sputter etching (but in marked contrast to Re(VI)); greater than 60% of the total oxidized component remained after 5 min bombardment, during which the surface Re(0) composition increased from 16.5% to 36.2%. In further contrast to the Re:Ru = 0.12 sample, the surface Re:Ru content of 0.43 is at greater variance with the initial stoichiometry used (0.54), which may be a consequence of a bimodal distribution of 8 nm and 2–4 nm Ru/Re particles determined for the system. The contrast between the final states of the two Ru/Re catalyst samples may be readily rationalized by a consideration of the different reactions involved in their genesis. Whereas cyclohexene hydrogenation over the Re:Ru = 0.12 catalyst occurs under essentially anhydrous conditions, amide hydrogenation with the Re:Ru = 0.54 catalyst requires the elimination of a stoichiometric amount of water during reduction, the presence of which presumably leads to the observed extensive oxidative hydrolysis of the Re surface.

3.7.3.2. Rh/Re catalysts. XPS data for the Re:Rh = 1.0 catalyst, both in the as-prepared form and after Ar^+ sputter etching, show that Rh is predominantly in the metallic state throughout, with a $3d_{5/2}$ binding energy of 307.2 eV, and no evidence of Rh_2O_3 (308.5 eV [1]). Curve fitting of the Re 4f data (see Supplementary material, Fig. S6 and Table 6) is consistent with the Re surface initially comprising three components, mainly Re(VI), together with Re(III) and Re(0), both oxidized states being removed completely by Ar^+ sputter etching for 1 min, at which point the surface Re:Rh composition is in close correspondence with the original stoichiometry used in catalyst preparation. After etching, no Rh 4p ($4p_{3/2}$ B.E. ~48 eV) intensity is evident, presumably due to the low sensitivity of the 4p signal.

XPS data on both Ru/Re and Rh/Re catalysts reveal that the Ru and Rh surfaces are essentially metallic, in sharp contrast to the Re components of the catalysts used in amide hydrogenation. In addition to Re(0), these contain significant amounts of higher valence states of Re, in the range Re(VII–III) with Ru, (VI and III) with Rh, and which, in the case of Ru, are resistant towards complete removal by Ar^+ bombardment, differences that are possibly attributable to the higher oxophilicity of Ru relative to Rh. An overlay of the Re 4f spectra of the three catalysts (see Supplementary material, Fig. S7) provides a direct comparison between the Ru/Re catalyst used for cyclohexene hydrogenation and the two used in amide reduction, clearly emphasizing the high levels of oxidized Re on the latter two, which may be indicative of an active role for such materials during amide reduction. In this context, reports of the use of Re-oxo complexes such as $[(OH)ReO_3]$ as catalysts for the dehydration of amides and aldoximes [19] could be significant in mechanistic terms (see Section 6).

4. Nature of the working catalysts

With Re:Ru and Re:Rh values obtained by ICP analysis in good agreement with those expected from the nominal precursor ratios, the Ru/Re- and Rh/Re-containing materials seem better defined

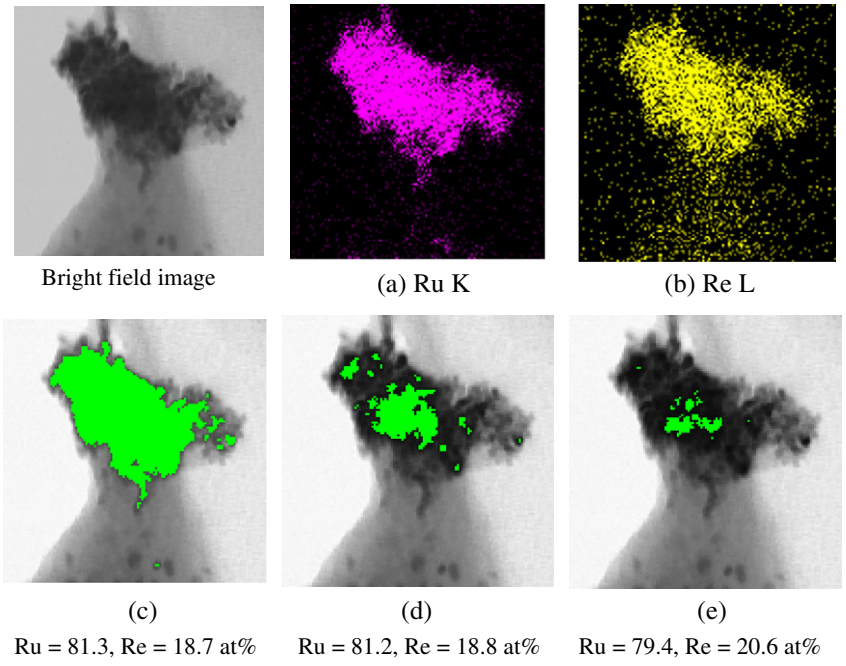

Fig. 8. EDX-STEM analysis of Re:Ru = 0.15 catalyst. (a) Ru K (19.279 keV) and (b) Re L (8.654 keV) maps. (c–e) Ru, Re quantification, areas of analysis depicted in light green. (For interpretation of the references to colour in this figure legend, the reader is referred to the web version of this article.)

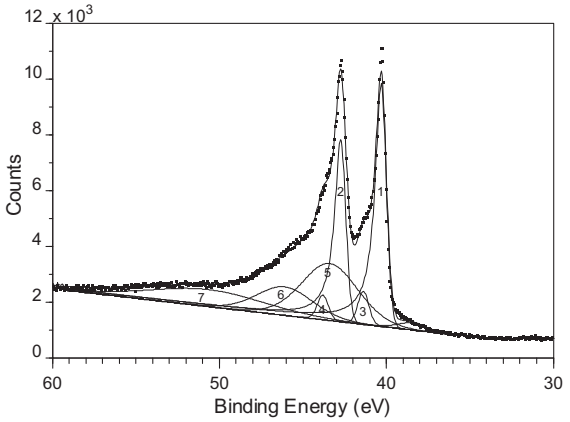

Fig. 9. XPS data: Curve fit to Re 4f region of Re:Ru = 0.12. Components 1, 2: Re(0) $4f_{7/2,\ 5/2}$; components 3, 4: Re(III) $4f_{7/2,\ 5/2}$; components 5, 6: Ru(0) $4p_{3/2,\ 1/2}$; component 7: Ru 4p satellite.

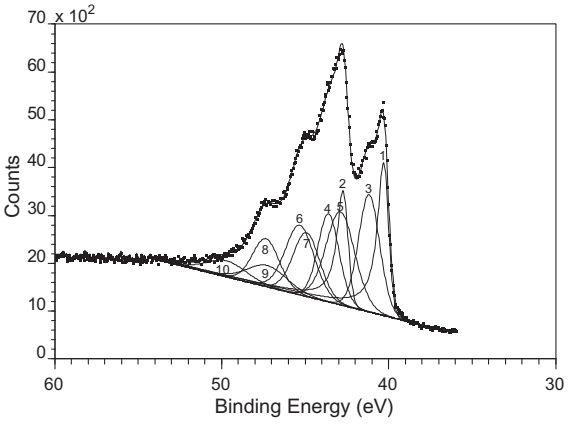

Fig. 10. XPS data: Curve fit to Re 4f region of Re:Ru = 0.54; components 1, 2: Re(0) $4f_{7/2,\ 5/2}$; components 3, 4: Re(III) $4f_{7/2,\ 5/2}$; components 5, 6: Re(IV) $4f_{7/2,\ 5/2}$; components 7, 8: Re(VI) $4f_{7/2,\ 5/2}$; components 9, 10: Re(VII) $4f_{7/2,\ 5/2}$.

than their Ru/Mo and Rh/Mo counterparts in terms of elemental composition. From XRD measurements, the Rh/Re catalysts contain ca. 3–4 nm aggregates, considerably smaller than those obtained using $Rh_6(CO)_{16}$ alone (as also found with Rh/Mo catalysts). In contrast, based on XRD evidence alone, the Ru/Re catalysts appear to comprise ca. 8-nm aggregates, as also found for Ru particles derived from $Ru_3(CO)_{12}$ alone. However, such Ru aggregates behave very poorly as catalysts for amide hydrogenation [2] and are therefore unlikely to be responsible for the highly selective reduction of $CyCONH_2$ to $CyCH_2NH_2$. We presume therefore that the dominant XRD pattern, interpreted in terms of 8 nm particles, must mask the smaller homogeneously mixed particles of Ru and Re revealed by the very much more sensitive EDX-STEM technique. As demonstrated by in situ HP-FTIR, the rapid degradation of $Ru_3(CO)_{12}$ coupled with the much slower decomposition of $Re_2(CO)_{10}$ must account for the co-formation of a mixture of the larger Ru particles, in tandem with catalytically active Ru/Re nanocluster generation.

5. Comparison between Ru/Mo, Ru/Re, Rh/Mo and Rh/Re catalysts

A comparison between the behaviour of Ru/Mo and Rh/Mo catalysts for amide reduction has been reported previously [2]. Substitution of Mo by Re has revealed a further dimension in terms of variations, and the key features of all the catalyst combinations investigated during this work are summarized in Table 7. Factors that appear common to all catalysts are (i) the synergistic behaviour between each pair of elements in promoting amide reduction under reaction conditions which encompass the ranges between 20 and 100 bar H_2 and 130 and 160 °C, (ii) intrinsic high selectivities of these catalysts towards hydrogenation of the primary amide $CyCONH_2$ to the primary amine $CyCH_2NH_2$, and (iii) their recyclability. Whereas Ru/Mo, Rh/Mo and Rh/Re are all comparable in exhibiting significant induction periods prior to initiation of catalysis, Ru/Re only requires heating to reaction temperature. A consequence is that the extremely rapid rate of decomposition of $Ru_3(CO)_{12}$, relative to $Re_2(CO)_{10}$, leads to a bimodal distribution of ca. 8-nm Ru crystallites and ca. 2–4-nm Ru/Re nanoclusters.

Table 6
XPS data. Quantification of Re:Ru = 0.12, Re:Ru = 0.54 and Re:Rh = 1.0 catalysts (M vs. Re%), and Re valence state distribution (%) as a function of Ar^+ sputter etching time at 3 keV.

Catalyst	Ar^+ sputter etch time (min)	M total (%)	Re total (%)	Re(0)	Re(III)	Re(IV)	Re(VI)	Re(VII)
Re:Ru = 0.12	0	87.8	12.2	86.9	13.1	–	–	–
	1	87.0	13.0	94.6	5.4	–	–	–
	5	87.9	12.1	92.6	7.4	–	–	–
Re:Ru = 0.54	0	70.0	30.0	16.5	26.9	29.0	18.5	9.2
	1	71.0	29.0	27.0	24.2	25.6	14.4	8.8
	5	70.0	30.0	36.2	23.2	22.6	8.8	9.1
Re:Rh = 1.0	0	27.7	72.3	27.1	31.4	–	41.4	–
	1	48.6	51.4	100	–	–	–	–
	3	40.6	59.4	100	–	–	–	–

Table 7
Comparison between bimetallic catalysts for amide hydrogenation.

	Ru/Mo	Rh/Mo	Ru/Re	Rh/Re
Optimum Mo:M′/Re:M′	0.5	0.55	0.3–1.5	0.8
$CyCH_2NH_2$ selectivity (%)	85	85	95	90
H_2 pressure range (bar)	20–100	20–100	50–100	50–100
Minimum temperature (°C)	140	130	160	150
Nature of active catalyst	Ru/Mo and Mo oxides	Rh and Mo oxides	Ru/Re and Re oxides	Rh/Re and Re oxides

Ru/Mo, Ru/Re, Rh/Mo and Rh/Re catalysts are comparable in requiring only small amounts of the second element i.e., Re and Mo, for high primary amine selectivities, although Rh/Re catalysts do require higher Re:Rh compositions to allow full amide conversion. Contrasting features that emerge from the substitution of Re for Mo are (i) little significant catalyst deactivation at high Re levels, possibly because oxides of Re are much more readily reduced to the metallic state than Mo oxides and (ii) the requirement for more severe reaction conditions, ca. 50–100 bar H_2 and 150–160 °C with Ru/Re and Rh/Re-containing catalysts (cf. 20 bar H_2, 150 °C with Ru/Mo catalysts). Minimum acceptable reaction conditions required by Ru/Mo and Ru/Re catalysts are 20/50 bar H_2 and 160 °C, respectively, with almost identical (84% vs. 81%) primary amine selectivities, and thus Ru/Mo catalysts appear preferable to their Ru/Re analogues, particularly in the light of a higher TON of 4.7 h^{-1} for Ru/Mo [2] vs. 1.9 h^{-1} with Ru/Re (see Section 3.6.1), in comparable experiments. Nevertheless, the *real* TON associated with Ru/Re nanoclusters may in fact be significantly higher when the co-presence of largely inactive 8-nm Ru particles is taken into account.

None of these catalysts require the customary co-addition of ammonia or amines to inhibit the formation of secondary and tertiary amine by-products. We previously commented on the formation of cyclohexanemethanol (in ca.14% selectivity) as the only detectable by-product from $CyCONH_2$ hydrogenation over Ru/Mo catalysts [2]. Slightly less (ca. 10%) appears to be the norm with the Re-containing systems reported here (with correspondingly slightly higher selectivities to $CyCH_2NH_2$). The formation of $CyCH_2OH$, presumably consequent upon C—N rather than C—O bond scission, requires the elimination of one equivalent of NH_3 per equivalent of $CyCONH_2$ consumed via this pathway (see Scheme 1), leading to the possibility that this internal generation of NH_3 might be sufficient to suppress $(CyCH_2)_2NH$ formation.

Although the bulk of this work has been undertaken using the zerovalent metal carbonyls $Ru_3(CO)_{12}$, $Rh_6(CO)_{16}$ and $Re_2(CO)_{10}$ as catalyst precursors, other more readily available sources of Ru, Rh and Re may also suffice. For Ru/Mo and Rh/Mo catalysts, the Mo(0) precursor $Mo(CO)_6$ appeared essential for both synergistic amide conversion and primary amine selectivity [1,2]. However, this limitation did not necessarily extend to Ru or Rh, where the Ru(III) precursor $Ru(acac)_3$ [and Rh(I) precursor $Rh(CO)_2(acac)$] (acac = acetylacetonato-, $[CH_3C(O)CHC(O)CH_3]^-$) were also shown to be effective. Oxides of rhenium are much more readily reduced to the metallic state than Mo oxides, cf. the in situ reduction of Re_2O_7 and OsO_4 to give the bimetallic Re/Os catalysts used in the hydrogenation of carboxylic acids [5,20]. A catalyst prepared using $Ru_3(CO)_{12}$ and Re_2O_7 was found to give $CyCH_2NH_2$ in 90% selectivity, at 100% conversion of $CyCONH_2$ [21], suggesting that in further work Re_2O_7 might represent a more convenient precursor than $Re_2(CO)_{10}$ to Re-containing catalysts for amide hydrogenation.

6. Comments on mechanistic steps involved in the reduction of amides

Notwithstanding extensive searching, we note an extreme paucity of information concerning mechanistic steps associated with the reduction of amide functional groups.

$$\mathrm{RCONR'R''} + 2\mathrm{H_2} \rightarrow \mathrm{RCH_2NR'R''} + \mathrm{H_2O}$$
$$\mathrm{R,R',R''} = \mathrm{H, alkyl\ or\ aryl, etc.} \quad (1)$$

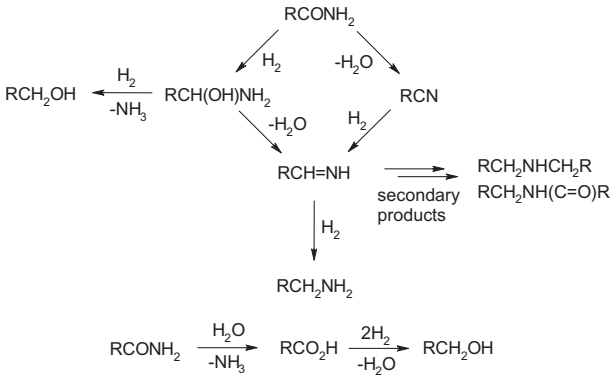

Scheme 1. Postulated alternative reaction pathways, and intermediates, in the reduction of primary amides.

Two principal pathways appear to suggest themselves (Scheme 1). First, addition of H_2 across the C=N bond of the thermodynamically strongly disfavoured iminol tautomer, which may nevertheless be kinetically significant, to give the carbinolamine (hemiaminal) would intuitively seem to be more favoured than direct addition of H_2 across the strongly deactivated C=O group of the amide. Addition of a second equivalent of hydrogen with concerted elimination of water would complete the reduction sequence. Alternatively, initial dehydration of the carbinolamine to the imine, followed by direct addition of hydrogen could also allow completion of the reduction sequence. A second 'reverse' pathway, available to primary amides, concerns initial dehydration of the amide to the corresponding nitrile, followed by sequential hydrogenation with two equivalents of hydrogen.

$$RCONH_2 \xrightarrow{-H_2O} RCN \xrightarrow{H_2} RCH = NH \xrightarrow{H_2} RCH_2NH_2 \quad (2)$$

Free energy changes for potential intermediates in the two alternative reduction pathways, for R = Cy, cyclohexyl, have been estimated using group additivity methods [22,23] and the results are summarized in Table 8. $\Delta G^{\circ}_{298.15}$ for the formation of the carbinolamine $CyCH(OH)NH_2$ from $CyCONH_2$ is estimated to be 104.8 kJ mol^{-1} (Entry 2) [23], a value far in excess of the amide dehydration barrier (Entry 4), suggesting that amide dehydration might actually provide a more favourable reaction pathway for the reduction of primary amides. The carbinolamine actually proves thermodynamically unstable with respect to imine formation and elimination of water, cf. Entries 2 and 3, thereby favouring this option over the alternative addition of H_2 and concerted elimination of water referred to above.

The operation of an amide dehydration pathway may clearly play a role in controlling the unusually high selectivity towards $CyCH_2NH_2$, because removal of water in the first step should inhibit $CyCH_2OH$ formation. Also, if dehydration to the nitrile were to be rate-limiting (considering the higher reaction temperatures, i.e.130–160 °C, required relative to those required by standard nitrile hydrogenation catalysts [24,25]), the low standing concentration of nitrile, and presumably very rapid subsequent reduction to amine, could reasonably be expected to lead to a limitation of secondary amine by-product formation, as observed experimentally.

Clearly both postulated mechanistic pathways may operate concurrently, but the potential availability of an additional route for primary amide reduction may perhaps also go some way towards providing an explanation for the demonstrated difference in reactivity of e.g., Ru/Mo catalysts towards primary, secondary and tertiary amide reduction, in the order $CyCONH_2 > CyCONMe_2 \gg CyCONHMe$ [2].

Whilst providing useful background information, the free energy estimates described above only give an idealistic representation of the reaction pathways because they do not take account of the effect of the requirement for adsorption of the reactants and intermediates (i.e. carbinolamine, imine) on the catalyst surface. In this context, it seems probable that a preferred orientation of the substrate on the catalyst surface would require adsorption of the amide N and carbonyl O at Ru/Rh and Re/Re oxide interfaces respectively. Concerted, or stepwise addition of H_2, the latter via the intermediacy of adsorbed $CyCH(O)NH_2$, would then lead to $CyCH_2NH_2$ formation and desorption. Removal of the co-formed chemisorbed O, as H_2O, by reaction with the second equivalent of H_2, would not only lead to catalyst regeneration but also invoke a role for redox behaviour on the surface during amide reduction. The contrasting nature of surface species associated with Ru/Re catalysts used for cyclohexene hydrogenation and amide reduction, as derived from XPS measurements (cf. Section 3.7.3), provides supporting circumstantial evidence for this possibility. Moreover, such behaviour may also account for the lack of a close correlation between amide and nitrile hydrogenation (see, Supplementary material S4) with similar catalysts. Here, very high primary amine selectivities were a feature of *both* monometallic and bimetallic CyCN hydrogenation catalysts examined (Ru, Ru/Re, Ru/Mo, Rh and Rh/Mo), in marked contrast to the behaviour of monometallic amide reduction catalysts. Also, the variable synergism observed with nitrile hydrogenation catalysts following the introduction of Re and Mo components may be a direct consequence of the 'anhydrous' nature of these systems and the absence of redox catalysis, thus rendering the amide and nitrile reduction systems incomparable in direct terms.

Finally, transient imine intermediates may be common to all mechanistic pathways, and some consideration of the evidence for their existence is appropriate. Imines have frequently been postulated, particularly in the context of intermediates in the reduction of nitriles [24,25], and the apparent lack of direct evidence for their existence attributed to high reactivity. Nevertheless, it is pertinent to note that coordinated imines have in fact been isolated and characterized during model studies in organometallic chemistry directed towards the definition of intermediate stages in the reduction of nitriles [26,27]. Moreover, using NMR spectroscopy, Fryzuk et al. [28] demonstrated the formation of bridged imines and their conversion to coordinated secondary amines during stoichiometric reactions of nitriles with Rh hydride-containing complexes. Here, temperatures as low as 77 K were required to monitor their reactions because of the extremely high lability of even these organometallic systems, in which the imine would be expected to be 'stabilized' by coordination, thus providing unequivocal confirmation of their extremely high reactivity. Thus, although there is little direct evidence for the involvement of imine intermediates, postulation of their transient existence certainly conveniently accounts for the formation of secondary and tertiary amine by-products commonly formed during the reduction of both amides (Scheme 1) and nitriles. Furthermore, the detection and unequivocal characterization of the secondary amide $Cy-C(O)N(CH_2Cy)H$ as a minor by-product during the reduction of $CyCONH_2$ over Rh/Mo catalysts [1] provides further circumstantial evidence in support of the transient existence of CyCH = NH.

7. Summary and conclusions

The use of recyclable, bimetallic Re-containing heterogeneous catalysts for highly selective reduction of the primary amide

Table 8
Thermodynamic parameters relevant to amide hydrogenation.

Entry	Reaction	ΔH° kJ mol^{-1}	ΔS° Jmol^{-1} K^{-1}	$\Delta G^{\circ}_{298.15}$ kJ mol^{-1}
1	$CyCONH_2 + 2H_2 \rightarrow CyCH_2NH_2 + H_2O$	−49.8	−72.8	−28.1
2	$CyCONH_2 + H_2 \rightarrow CyCH(OH)NH_2$	51.5	−178.7	104.8
3	$CyCONH_2 + H_2 \rightarrow CyCH = NH + H_2O$	63.2	−21.1	69.5
4	$CyCONH_2 \rightarrow CyCN + H_2O$	73.2	156.5	26.5
5	$CyCN + H_2 \rightarrow CyCH = NH$	−10.0	−177.6	43.0
6	$CyCH = NH + H_2 \rightarrow CyCH_2NH_2$	−113.0	−51.7	−97.6
7	$CyCN + 2H_2 \rightarrow CyCH_2NH_2$	−123.0	−229.7	−54.6

$CyCONH_2$, in the liquid phase, to the corresponding primary amine, $CyCH_2NH_2$, has been demonstrated for the first time. These Ru/Re and Rh/Re catalysts are effective under considerably milder reaction conditions than those required by earlier generation catalysts such as copper chromite. The new nanocluster catalysts, prepared in situ from the parent metal carbonyls, have only been investigated in the unsupported state, whereas supported catalysts would clearly be preferable for larger scale use. Our preliminary attempts to support related Rh/Mo catalysts proved largely unsuccessful, notwithstanding their displaying higher initial TONs in amide reduction than the unsupported materials [1]. This was a consequence of accumulation of C, H and N residues on the silica support used during recycling, resulting in very significant deactivation. Future work in this area should be directed towards this aspect, with careful attention to the selection and use of alternative supports, e.g. high surface area carbon, or possibly other reducible oxides such as titania [6]. The use of more readily available catalyst precursors than the metal carbonyls, e.g. $[Ru(acac)_3]$, Re_2O_7 and $[Rh(CO)_2(acac)]$, may also prove advantageous. Furthermore, the general approach should be extended towards secondary amides, the hydrogenation of which appears to be considerably more difficult than primary amides in both catalytic and stoichiometric reactions (the latter using hydride reagents such as $LiAlH_4$ [2], and references therein). In contrast, reduction of the tertiary amides that are commonly used as models of amide hydrogenation, e.g. *N*-acetylpiperidine and *N*-acetylpyrrolidine, is generally trivial, principally because amine product selectivity only poses a minor problem, certainly with the bimetallic catalysts described here. Other functional groups that are well known for their difficult reducibility include carboxylic acids and esters, and these may also be accessible to these catalysts. Finally, significant recent reports of the reduction of amides to the corresponding amines (and alcohols) under mild reaction conditions include the use of homogeneous bipyridyl-based Ru [29], Fe and Zn/triethoxysilane-mediated [30] catalysts, indicative of a resurgence of interest in this challenging area.

Acknowledgments

The authors acknowledge helpful discussions with Dr. J. Claridge and Dr. J.A. Iggo (Department of Chemistry) and Mr. A.J. Pettman (Pfizer Ltd.), EPSRC for financial support of NCESS, Daresbury, under grant GR/S14252/01, and the Leverhulme Fine Chemicals Forum for financial support (to C.P. and A.M.S.).

Appendix A. Supplementary material

Supplementary data associated with this article can be found, in the online version, at doi:10.1016/j.jcat.2010.12.009.

References

[1] G. Beamson, A.J. Papworth, C. Philipps, A.M. Smith, R. Whyman, J. Catal. 269 (2010) 93–102.
[2] G. Beamson, A.J. Papworth, C. Philipps, A.M. Smith, R. Whyman, Adv. Synth. Catal. 352 (2010) 869–883.
[3] B. Wojcik, H. Adkins, J. Am. Chem. Soc. 56 (1934) 247; 2419–2424.
[4] H.S. Broadbent, G.C. Campbell, W.J. Bartley, J.H. Johnson, J. Org. Chem. 24 (1959) 1847–1854.
[5] K. Yoshino, Y. Kajiwara, N. Takaishi, Y. Inamoto, J. Tsuji, J. Am. Oil Chem. Soc. 67 (1990) 21–24.
[6] H.G. Manyar, C. Paun, R. Pilus, D.W. Rooney, J.M. Thompson, C. Hardacre, Chem. Commun. 46 (2010) 6279–6281.
[7] H.S. Broadbent, W.J. Bartley, J. Org. Chem. 28 (1963) 2345–2347.
[8] I.D. Dobson, Eur. Patent, 286 280, 1988 (to BP).
[9] C. Hirosawa, N. Wakasa, T. Fuchikami, Tet. Lett. 37 (1996) 6749–6752.
[10] M. Balcerzak, Crit. Rev. Anal. Chem. 32 (2002) 181–226.
[11] J.R. Johnson, H.D. Kaesz, Inorg. Synth. 18 (1978) 60–62.
[12] M. Herberhold, G. Süss, J. Ellerman, H. Gäblein, Chem. Ber. 111 (1978) 2931–2941.
[13] A. Davison, J.A. McCleverty, G. Wilkinson, J. Chem. Soc. (1963) 1133–1138.
[14] S. Martinengo, P. Chini, Gazz. Chim. Ital. 102 (1972) 344–354.
[15] H.E. Swanson, R.K. Fuyat, Natl. Bur. Stand. (US) Circ 539, vol. II, 1953, p. 13.
[16] A. Cimino, B.A. De Angelis, D. Gazzoli, M. Valegi, Z. Anorg. Allg. Chem. 460 (1980) 86–98.
[17] W. Geilmann, F.W. Wrigge, Z. Anorg. Chem. 214 (1933) 239–243.
[18] G.J. Leigh, W. Bremser, J. Chem. Soc. Dalton Trans. (1972) 1216–1219.
[19] K. Ishihara, Y. Furuya, H. Yamamoto, Angew. Chem. Internat. Edit. 16 (2002) 2983–2986.
[20] C. Philipps, Ph.D. Thesis, University of Liverpool, 2004.
[21] A.M. Smith, Ph.D. Thesis, University of Liverpool, 2006.
[22] S.E. Stein, R.L. Brown, "Structures and Properties Group Additivity Model" in NIST chemistry WebBook, NIST standard reference database number 69, in: P.J. Linstrom, W.G. Mallard (Eds.), March 2003, National Institute of Standards and Technology, Gaithersburg, MD, 20899. http://webbook.nist.gov.
[23] S.W. Benson, Thermochemical Kinetics: Methods for the Estimation of Thermochemical Data and Rate Parameters, John Wiley & Sons, New York, 1968.
[24] S. Nishimura, Handbook of Heterogeneous Catalytic Hydrogenation for Organic Synthesis, John Wiley and Sons, New York, 2001 (and references therein).
[25] J. Volf, J. Pašek, Catalytic hydrogenation, in: L. Cerverny (Ed.), Elsevier Science, Amsterdam, 1986, pp. 105–145.
[26] M.A. Andrews, H.D. Kaesz, J. Am. Chem. Soc. 101 (1979) 7255–7259.
[27] Z. Dawoodi, M.J. Mays, K. Henrick, J. Chem. Soc. Dalton Trans. (1984) 433–440.
[28] M.D. Fryzuk, W.E. Piers, S.J. Rettig, Can. J. Chem. 70 (1992) 2381–2389.
[29] E. Balaraman, B. Gnanaprakasam, L.J.W. Shimon, D. Milstein, J. Am. Chem. Soc. 132 (2010) 16756–16758.
[30] S. Das, S. Zhou, D. Addis, S. Enthaler, K. Junge, M. Beller, Top. Catal. 53 (2010) 979–984.